Low Complexity Multi-mode Signal Detection for DTMB System

Xue Liu(✉), Guido H. Bruck, and Peter Jung

Department of Communication Technologies,
University of Duisburg-Essen, Duisburg, Germany
{xue.liu,guido.bruck,peter.jung}@kommunikationstechnik.org

Abstract. The Digital Terrestrial Multimedia Broadcast (DTMB) system utilizes three modes of Pseudo-noise (PN) sequences as Frame Header (FH) that can be exploited for spectrum sensing on TV White Space (TVWS). As a consequence, multi-mode signal detection is required at the receiver. In this paper, Neyman-Person (NP) lemma based, Multi-mode Local Sequence (MLS) detectors are proposed for multi-mode signal detection. The theoretical and quantitative performance analysis of MLS detectors are mainly concentrated and fully studied by utilizing the addition and auto-correlation properties of PN sequence. In addition, the single-mode detector for the DTMB system is presented as the optimal detector and taken as a benchmark for MLS detectors. Both theoretical analyses and simulation results show that MLS detectors are capable of multi-mode signal detection and satisfy the predefined sensing requirements.

Keywords: Digital terrestrial multimedia broadcast · TV white space · Spectrum sensing · Pseudo-noise sequence

1 Introduction

TV White Space (TVWS) refers to the frequency band where the radio spectrum is not used by primary users [4]. It can be potentially accessed by secondary users via Cognitive Radio (CR) [7], which results in increased overall spectrum efficiency and innovative new services. The requirement for TVWS spectrum sensing allows the coexistence of secondary users without harmful interference to primary users. For instance, the sensing requirements for the Advanced Television Systems Committee (ATSC) system [8] defined by IEEE 802.22 [2] are as low as −21 dB within 20 ms sensing time when the false-alarm probability (P_{FA}) is below 10% and the detection probability (P_{D}) is above 90%.

Digital Terrestrial Multimedia Broadcast (DTMB) is a Chinese digital terrestrial television standard [1,9]. Applying spectrum sensing for the DTMB system can extend the application of TVWS. Although specific requirements for the DTMB spectrum sensing are not available so far, the same requirements of the ATSC system are also adequate for the DTMB system.

M. Weichold et al. (Eds.): CROWNCOM 2015, LNICST 156, pp. 271–281, 2015.
DOI: 10.1007/978-3-319-24540-9_22

The DTMB system specifies three major modes of Pseudo-noise (PN) sequences padding with PN420/595/945 as Frame Header (FH) which is shown in Figure 1. They can be utilized for signal synchronization and channel estimation at the receiver. Several detectors have been derived, which exploited properties of PN sequence, for example the auto-correlation detector is proposed in [3], and in [10] the cross-correlation property is employed. The detector proposed in [6] is an extension of an auto-correlation detector. It takes advantage of max-mean-ratio as test statistic that is a true constant false-alarm rate (CFAR) detector owing to its "self-normalizing" feature, which removes the dependence on the noise power. All the aforementioned algorithms are designated for single-mode signal. They are not capable of detecting multi-mode signals. Therefore a low time complexity and implementation-friendly detector for multi-mode signals is necessary for the DTMB system, which is the main focus of this manuscript.

In this paper, we focus on the spectrum sensing algorithm for DTMB multi-mode signals. By exploiting addition and auto-correlation properties of PN sequence, two Multi-mode Local Sequence (MLS) combination schemes are proposed and analyzed quantitatively in detail. Theoretical analysis and simulation results show that MLS detectors can achieve multi-mode signal detection with a tolerable loss of sensing performance.

The rest of this paper is organized as what follows. The single-mode signal detector for DTMB system is introduced in Section 2. MLS based multi-mode signal detection methodologies are analyzed in detail in Section 3. The simulation results are demonstrated in Section 4. Finally Section 5 concludes the manuscript.

2 Single-Mode Signal Detector

In what follows, the optimal detector of single-mode signal is derived from first principles. Regarding a known deterministic signal for Additive White Gaussian Noise (AWGN) scenario, the optimal detector is Neyman-Person (NP) test, known as matched filter [5].

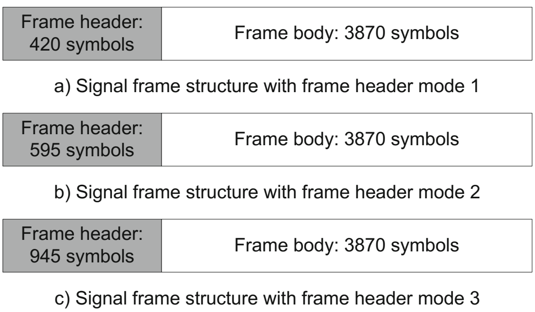

Fig. 1. Frame structure of DTMB system

Let $\mathcal{H}_0$ be the null hypothesis, i.e., a primary user is absent, and $\mathcal{H}_1$ be the alternate hypothesis, i.e., DTMB signals presence. Therefore, the hypothesis testing problem can be written as

$$\mathcal{H}_1 : \underline{\boldsymbol{r}}_i = \underline{\boldsymbol{c}}_i + \underline{\boldsymbol{n}}_i, \qquad i = 0, 1, \ldots, N-1, \tag{1}$$

$$\mathcal{H}_0 : \underline{\boldsymbol{r}}_i = \underline{\boldsymbol{n}}_i, \qquad i = 0, 1, \ldots, N-1, \tag{2}$$

where $\underline{\boldsymbol{c}}$ denotes one of original three modes PN sequences. N is the number of received signal frames. $\underline{\boldsymbol{r}}_i$ denotes the received signal vector. $\underline{\boldsymbol{n}}_i$ denotes the AWGN vector and it is a complex circularly symmetric Gaussian random variable with distribution $\mathcal{CN}(\mathbf{0}, \sigma_n^2 \mathbf{I})$.

The NP detector is in favors of $\mathcal{H}_1$ if the Likelihood Ratio Test (LRT) exceeds a threshold, like

$$L(\underline{\boldsymbol{r}}) = \frac{p(\underline{\boldsymbol{r}}; \mathcal{H}_1)}{p(\underline{\boldsymbol{r}}; \mathcal{H}_0)} > \gamma. \tag{3}$$

Since

$$p(\underline{\boldsymbol{r}}; \mathcal{H}_1) = \frac{1}{(\pi\sigma_n^2)^{NM}} \exp\left[-\frac{1}{\sigma_n^2} \sum_{i=0}^{N-1} \| \underline{\boldsymbol{r}}_i - \underline{\boldsymbol{c}}_i \|^2 \right], \tag{4}$$

and

$$p(\underline{\boldsymbol{r}}; \mathcal{H}_0) = \frac{1}{(\pi\sigma_n^2)^{NM}} \exp\left[-\frac{1}{\sigma_n^2} \sum_{i=0}^{N-1} \| \underline{\boldsymbol{r}}_i \|^2 \right], \tag{5}$$

we have

$$T(\underline{\boldsymbol{r}}) = \frac{1}{\sigma_n^2} \sum_{i=0}^{N-1} \Re\left(\underline{\boldsymbol{c}}_i^{\mathrm{H}} \underline{\boldsymbol{r}}_i \right) > \ln\gamma + \frac{N\varepsilon}{2\sigma_n^2}, \tag{6}$$

$$\Rightarrow T(\underline{\boldsymbol{r}}) = \sum_{i=0}^{N-1} \Re\left(\underline{\boldsymbol{c}}_i^{\mathrm{H}} \underline{\boldsymbol{r}}_i \right) \geq \gamma'. \tag{7}$$

where ε is the energy of $\underline{\boldsymbol{c}}$. $T(\underline{\boldsymbol{r}})$ is the test statistic of optimal detector of single-mode signal.

Thus, under both hypotheses, the distribution of $T(\underline{\boldsymbol{r}})$ is given by

$$T(\underline{\boldsymbol{r}}) \sim \begin{cases} \mathcal{N}\left(0, N\sigma_n^2\varepsilon/2\right) & \text{under } \mathcal{H}_0 \\ \mathcal{N}\left(N\varepsilon, N\sigma_n^2\varepsilon/2\right) & \text{under } \mathcal{H}_1. \end{cases} \tag{8}$$

Therefore, P_{FA} and P_{D} can be derived from (8), and shown below,

$$P_{\mathrm{FA}} = \Pr\{T > \gamma'; \mathcal{H}_0\} = \mathrm{Q}\left(\frac{\gamma'}{\sqrt{N\sigma_n^2\varepsilon/2}} \right) \tag{9}$$

$$P_{\rm D} = \Pr\{T > \gamma'; \mathcal{H}_1\} = \mathrm{Q}\left(\frac{\gamma' - N\varepsilon}{\sqrt{N\sigma_n^2 \varepsilon/2}}\right), \tag{10}$$

where Q is the right-tail probability function of the standard normal distribution. The new threshold is derived by

$$\gamma' = \sqrt{\frac{N\sigma_n^2\varepsilon}{2}} \mathrm{Q}^{-1}\left(P_{\rm FA}\right). \tag{11}$$

Substituting (11) to (10), we have

$$P_{\rm D} = \mathrm{Q}\left(\mathrm{Q}^{-1}\left(P_{\rm FA}\right) - \sqrt{\frac{2N\varepsilon}{\sigma_n^2}}\right). \tag{12}$$

It is known that $N\varepsilon/\sigma_n^2$ is Energy Noise Ratio (ENR) [5]. It presents the ratio between the whole energy from received signal and the noise power spectrum density.

3 Multi-mode Signal Detector

In this section, multi-mode detectors are derived from the NP test for AWGN scenario. The key observations for deducing the multi-mode detector are the addition and auto-correlation properties of PN sequence. In the DTMB system, PN255 and PN511 sequences are cyclically extended to sequences of length 420 and 945 for Mode 1 and Mode 3 frames, respectively. Due to reduction of the analysis and time complexity, only PN255, PN511 and PN595 are utilized for MLS design.

3.1 Multi-mode Local Sequence Design

PN sequences are quasi-orthogonal, which means

$$\frac{\underline{\boldsymbol{c}}_i(p)^{\rm H}\underline{\boldsymbol{c}}_j(q)}{M} \approx \begin{cases} 1 & p = q \text{ and } i = j \\ 0 & \text{others,} \end{cases} \tag{13}$$

where M is the length of $\underline{\boldsymbol{c}}$, $\underline{\boldsymbol{c}}_i(p)$, $\underline{\boldsymbol{c}}_j(q)$ are different PN sequences from different modes and with different phases. Based on this observation, three different multi-mode local sequences with serial, parallel, and mixed structures are introduced for the DTMB system [11] below.

The structure of Serial Multi-Mode Local Sequence (SMLS) is shown in Figure 2 and its vector form is represented as

$$\underline{\boldsymbol{c}}_{\rm S} = \begin{bmatrix} \underline{\boldsymbol{c}}_1 \\ \underline{\boldsymbol{c}}_2 \\ \underline{\boldsymbol{c}}_3 \end{bmatrix}. \tag{14}$$

Fig. 2. Structure of serial multi-mode local Sequence

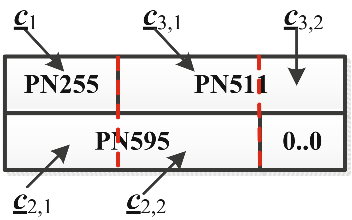

Fig. 3. Structure of mix multi-mode local sequence

For ease of notation and calculation, the MLS is divided into different parts. The structure of Mix Multi-mode Local Sequence (MMLS) is shown in Figure 3, and its vector form is represented as

$$\underline{c}_{\mathrm{M}} = \begin{bmatrix} \underline{c}_1 + \underline{c}_{2,1} \\ \underline{c}_{3,1} + \underline{c}_{2,2} \\ \underline{c}_{3,2} + \mathbf{0} \end{bmatrix}. \tag{15}$$

Similarly, the Parallel Multi-mode Local Sequence (PMLS) is also divided into parts and shown in Figure 4 and its vector form is represented as

$$\underline{c}_{\mathrm{P}} = \begin{bmatrix} \underline{c}_1 + \underline{c}_{2,1} + \underline{c}_{3,1} \\ \underline{c}_{2,2} + \underline{c}_{3,2} + \mathbf{0} \\ \underline{c}_{2,3} + \mathbf{0} \end{bmatrix}, \tag{16}$$

where $\underline{c}_1$ and $\underline{c}_2$ must be padded with $\mathbf{0}$ until the same length as $\underline{c}_3$.

Since the mount of calculation is proportional to the length of sequence, the SMLS has the same time complexity as parallel single-mode detectors, which is not satisfied with the requirement of time complexity and therefore analysis and simulation of the SMLS detector is left out.

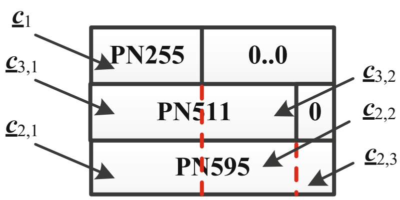

Fig. 4. Structure of parallel multi-mode local sequence

Under either hypothesis, $\underline{\boldsymbol{r}}_i$ is still Gaussian variable and $T(\underline{\boldsymbol{r}})$ satisfies the requirement of NP test, which can be utilized for multi-mode signal detection.

3.2 Mix Multi-mode Local Sequence Detector

Under $\mathcal{H}_0$, received signal contains only noise. According to (7), inner product of MMLS and received signal vector is defined as

$$\langle \underline{\boldsymbol{r}}^*, \underline{\boldsymbol{c}}_{\mathrm{M}} \rangle = \underline{\boldsymbol{n}}^{\mathrm{H}} \begin{bmatrix} \underline{\boldsymbol{c}}_1 + \underline{\boldsymbol{c}}_{2,1} \\ \underline{\boldsymbol{c}}_{3,1} + \underline{\boldsymbol{c}}_{2,2} \\ \underline{\boldsymbol{c}}_{3,2} + \mathbf{0} \end{bmatrix}. \tag{17}$$

Substituting (17) to (7), test statistic is given as,

$$\begin{aligned} T_{\mathrm{M}}(\underline{\boldsymbol{n}}) &= \sum_{i=0}^{N-1} \Re\left(\underline{\boldsymbol{n}}_i^{\mathrm{H}} \underline{\boldsymbol{c}}_{\mathrm{M}}\right) \\ &= \sum_{i=0}^{N-1} \Re \begin{pmatrix} \underline{\boldsymbol{n}}_{i,1}^{\mathrm{H}} \underline{\boldsymbol{c}}_1 + \underline{\boldsymbol{n}}_{i,1}^{\mathrm{H}} \underline{\boldsymbol{c}}_{2,1} \\ + \underline{\boldsymbol{n}}_{i,2}^{\mathrm{H}} \underline{\boldsymbol{c}}_{3,1} + \underline{\boldsymbol{n}}_{i,2}^{\mathrm{H}} \underline{\boldsymbol{c}}_{2,2} \\ + \underline{\boldsymbol{n}}_{i,3}^{\mathrm{H}} \underline{\boldsymbol{c}}_{3,2} + \underline{\boldsymbol{n}}_{i,3}^{\mathrm{H}} \mathbf{0} \end{pmatrix}. \end{aligned} \tag{18}$$

Under $\mathcal{H}_0$, we have

$$\mathrm{E}\left(T_{\mathrm{M}}(\underline{\boldsymbol{n}}); \mathcal{H}_0\right) = 0 \tag{19}$$

$$\mathrm{Var}\left(T_{\mathrm{M}}(\underline{\boldsymbol{n}}); \mathcal{H}_0\right) = 1491 N \sigma_n^2. \tag{20}$$

The $T_{\mathrm{M}}(\underline{\boldsymbol{n}})$ consists of both auto-correlation of single mode PN sequence and its cross-correlation of other overlapping sequences. In addition, for the given MMLS, and referencing to (11), the threshold is fixed for different modes of signal.

Under $\mathcal{H}_1$, taking Mode 2 signals as the primary signal, each received signal consists of noise, a Mode 2 PN sequence and some data from frame body. The structure of MMLS and received Mode 2 signal is shown in Figure 5. Similarly, inner product of MMLS and received signal is defined as

$$\langle \underline{\boldsymbol{r}}^*, \underline{\boldsymbol{c}}_{\mathrm{M}} \rangle = \begin{bmatrix} \underline{\boldsymbol{c}}_{2,1} + \underline{\boldsymbol{n}}_1 \\ \underline{\boldsymbol{c}}_{2,2} + \underline{\boldsymbol{n}}_2 \\ \underline{\boldsymbol{d}} + \underline{\boldsymbol{n}}_3 \end{bmatrix}^{\mathrm{H}} \begin{bmatrix} \underline{\boldsymbol{c}}_1 + \underline{\boldsymbol{c}}_{2,1} \\ \underline{\boldsymbol{c}}_{3,1} + \underline{\boldsymbol{c}}_{2,2} \\ \underline{\boldsymbol{c}}_{3,2} + \mathbf{0} \end{bmatrix}. \tag{21}$$

From (21), test statistic $T_{\mathrm{M}}(\underline{\boldsymbol{r}})$ for Mode 2 signal can be derived and defined as

$$\begin{aligned} T_{\mathrm{M}}(\underline{\boldsymbol{r}}) &= \sum_{i=0}^{N-1} \Re\left(\underline{\boldsymbol{r}}_i^{\mathrm{H}} \underline{\boldsymbol{c}}_{\mathrm{M}}\right) \\ &= \sum_{i=0}^{N-1} \Re \begin{pmatrix} \left[\underline{\boldsymbol{c}}_{2,1} + \underline{\boldsymbol{n}}_1\right]^{\mathrm{H}} \left[\underline{\boldsymbol{c}}_1 + \underline{\boldsymbol{c}}_{2,1}\right] \\ + \left[\underline{\boldsymbol{c}}_{2,2} + \underline{\boldsymbol{n}}_2\right]^{\mathrm{H}} \left[\underline{\boldsymbol{c}}_{3,1}^{\mathrm{H}} + \underline{\boldsymbol{c}}_{2,2}\right] \\ + \left[\underline{\boldsymbol{d}} + \underline{\boldsymbol{n}}_2\right]^{\mathrm{H}} \left[\underline{\boldsymbol{c}}_{3,2} + \mathbf{0}\right] \end{pmatrix}. \end{aligned} \tag{22}$$

Therefore, we have

$$\mathrm{E}\left(T_{\mathrm{M}}\left(\underline{\boldsymbol{r}}\right);\mathcal{H}_1\right)=660N. \tag{23}$$

The mean value of $T_{\mathrm{M}}\left(\underline{\boldsymbol{r}}\right)$ consists of the real part of auto-correlation of PN595 and its correlation value with PN255 and part of PN511. By the similar deviation, we have

$$\mathrm{Var}\left(T_{\mathrm{M}}\left(\underline{\boldsymbol{r}}\right);\mathcal{H}_0\right)=1491N\sigma_n^2+353550N. \tag{24}$$

Note that multi-mode detectors work in a very low Signal Noise Ratio (SNR) scenario, where energy of signal is much lower than σ_n^2, which means that the variance of test statistic under $\mathcal{H}_1$ can be estimate by its variance under $\mathcal{H}_0$.

Finally, distributions of test statistic $T_{\mathrm{M}}\left(\underline{\boldsymbol{r}}\right)$ for two hypotheses are shown below.

$$T_{\mathrm{M}}\left(\underline{\boldsymbol{r}}\right)\sim\begin{cases}\mathcal{N}\left(0,1491N\sigma_n^2\varepsilon\right) & \text{under } \mathcal{H}_0\\ \mathcal{N}\left(660N,1491N\sigma_n^2\varepsilon\right) & \text{under } \mathcal{H}_1.\end{cases} \tag{25}$$

3.3 Parallel Multi-mode Local Sequence Detector

Under $\mathcal{H}_0$, each received signal contains only noise. According to (7), inner product of PMLS and received signal vector is defined as

$$\left\langle\underline{\boldsymbol{r}}^*,\underline{\boldsymbol{c}}_{\mathrm{P}}\right\rangle=\underline{\boldsymbol{n}}^{\mathrm{H}}\left(\begin{bmatrix}\underline{\boldsymbol{c}}_1\\ \mathbf{0}\end{bmatrix}+\begin{bmatrix}\underline{\boldsymbol{c}}_{3,1}\\ \underline{\boldsymbol{c}}_{3,2}\\ \mathbf{0}\end{bmatrix}+\begin{bmatrix}\underline{\boldsymbol{c}}_{2,1}\\ \underline{\boldsymbol{c}}_{2,2}\\ \underline{\boldsymbol{c}}_{2,3}\end{bmatrix}\right). \tag{26}$$

By the similar deviation, we have

$$\mathrm{E}\left(T_{\mathrm{P}}\left(\underline{\boldsymbol{n}}\right);\mathcal{H}_0\right)=0 \tag{27}$$

$$\mathrm{Var}\left(T_{\mathrm{P}}\left(\underline{\boldsymbol{n}}\right);\mathcal{H}_0\right)=1440N\sigma_n^2. \tag{28}$$

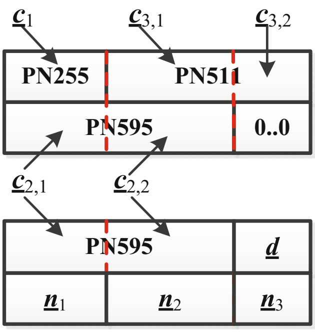

Fig. 5. Mix multi-mode local sequence and received DTMB Mode 2 signal, where each received signal consists of three parts, PN595, data frame and noise, which is divide into three vectors.

Likewise, the variance of $T_{\mathrm{P}}(\underline{\boldsymbol{n}})$ consists of both auto-correlation of PN595 and its cross-correlation of overlapping sequences from PN255 and PN511. In addition, the threshold for PMLS is also unique, which leads to a fix threshold for different modes of signal.

Under hypothesis $\mathcal{H}_1$, taking Mode 2 signal as primary signal. Similarly, inner product of PMLS and received signal is defined as

$$\langle \underline{\boldsymbol{r}}^*, \underline{\boldsymbol{c}}_{\mathrm{P}} \rangle = \begin{bmatrix} \underline{\boldsymbol{c}}_{2,1} + \underline{\boldsymbol{n}}_1 \\ \underline{\boldsymbol{c}}_{2,2} + \underline{\boldsymbol{n}}_2 \\ \underline{\boldsymbol{c}}_{2,3} + \underline{\boldsymbol{n}}_3 \end{bmatrix}^{\mathrm{H}} \left(\begin{bmatrix} \underline{\boldsymbol{c}}_1 \\ \mathbf{0} \end{bmatrix} + \begin{bmatrix} \underline{\boldsymbol{c}}_{3,1} \\ \underline{\boldsymbol{c}}_{3,2} \\ \mathbf{0} \end{bmatrix} + \begin{bmatrix} \underline{\boldsymbol{c}}_{2,1} \\ \underline{\boldsymbol{c}}_{2,2} \\ \underline{\boldsymbol{c}}_{2,3} \end{bmatrix} \right). \tag{29}$$

Substituting (29) to (7), test statistic $T_{\mathrm{P}}(\underline{\boldsymbol{r}})$ for Mode 2 signal is shown as

$$\begin{aligned} T_{\mathrm{P}}(\underline{\boldsymbol{r}}) &= \sum_{i=0}^{N-1} \Re \left(\underline{\boldsymbol{r}}_i^{\mathrm{H}} \underline{\boldsymbol{c}}_{\mathrm{P}} \right) \\ &= \sum_{i=0}^{N-1} \Re \left(\begin{array}{l} \left[\underline{\boldsymbol{c}}_{2,1} + \underline{\boldsymbol{n}}_1\right]^{\mathrm{H}} \left[\underline{\boldsymbol{c}}_1 + \underline{\boldsymbol{c}}_{2,1} + \underline{\boldsymbol{c}}_{3,1}\right] \\ \quad + \left[\underline{\boldsymbol{c}}_{2,2} + \underline{\boldsymbol{n}}_2\right]^{\mathrm{H}} \left[\underline{\boldsymbol{c}}_{3,2} + \underline{\boldsymbol{c}}_{2,2}\right] \\ \quad + \left[\underline{\boldsymbol{c}}_{2,3} + \underline{\boldsymbol{n}}_2\right]^{\mathrm{H}} \underline{\boldsymbol{c}}_{2,3} \end{array} \right). \end{aligned} \tag{30}$$

By the similar derivation, we have

$$\mathrm{E}\left(T_{\mathrm{P}}(\underline{\boldsymbol{r}}); \mathcal{H}_1\right) = 630N \tag{31}$$

$$\mathrm{Var}\left(T_{\mathrm{P}}(\underline{\boldsymbol{r}}); \mathcal{H}_1\right) = 1440N\sigma_n^2 + 350150N. \tag{32}$$

Finally, with the same estimation of variance above under $\mathcal{H}_1$, the distributions of test statistic $T_{\mathrm{P}}(\underline{\boldsymbol{r}})$ for two hypotheses are shown below.

$$T_{\mathrm{P}}(\underline{\boldsymbol{r}}) \sim \begin{cases} \mathcal{N}\left(0, 1440N\sigma_n^2\varepsilon\right) & \text{under } \mathcal{H}_0 \\ \mathcal{N}\left(630N, 1440N\sigma_n^2\varepsilon\right) & \text{under } \mathcal{H}_1. \end{cases} \tag{33}$$

4 Simulation Results

To show the overall performance of previously introduced algorithms, signal sensitivity comparisons between multi-mode detectors and single-mode detectors are given via Monte Carlo simulations. Simulation parameters are showed in Table 1.

The Receiver Operating Characteristic (ROC) curve for DTMB Mode 1 signal is shown in Figure 6, which indicates that the signal sensitivity of both MMLS and PMLS detectors is close but still worse that of signal-mode detector. The reason of such degradations could owing to the quasi-orthogonal property of the PN sequence with finite length. It will results in the decrease of ENR.

The signal sensitivity in terms of probability of detection over SNR is depicted in Figure 7 and Figure 8. For DTMB Mode 2 signals, taking 20 signal frames,

Table 1. Simulation parameters

Parameter	Value
Signal mode	PN255, PN511, PN595
Number of received frames	20
Target probability of false-alarm	10%
Propagation channel	AWGN

the single-mode detector can achieve the signal sensitivity in term of SNR as low as −35.43 dB and $P_{\mathrm{MD}} = 10\%$. In the same situation, MMLS and PMLS detectors are capable of −32.67 dB and −31.81 dB, respectively. For DTMB Mode 1 signals, taking the same number of received frames, a sensitivity of −32.09 dB, −22.09 dB and −19.09 dB can be reached by single-mode detector, MMLS and PMLS detectors, respectively when $P_{\mathrm{MD}} = 10\%$. The sensing time of 20 frames takes approximately 11 ms, which is much less than the predefined 20 ms. Therefore the sensing performance of both multi-mode detectors can satisfy the predefined sensitivity requirements of the DTMB system.

All the figures show that the MMLS detector has slight better sensing performance than PMLS detector. The reason is that the MMLS has larger ENR under $\mathcal{H}_1$. According to the discussion in Section 2, the ENR is proportional to the ratio of mean value and variance of test statistic. For Mode 2 signal, from distributions given in (25) and (33), we can find that the ratio of MMLS is 0.442 that is larger than 0.4375 of PMLS.

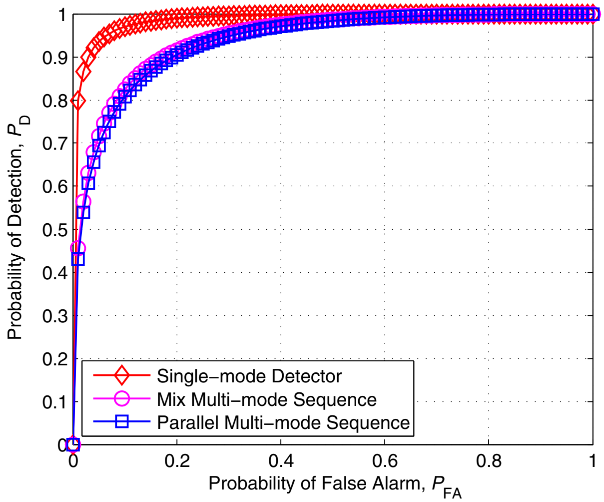

Fig. 6. ROC curves of single-mode detector, MMLS detector and PMLS detector for DTMB Mode 1 signal when SNR = −34 dB.

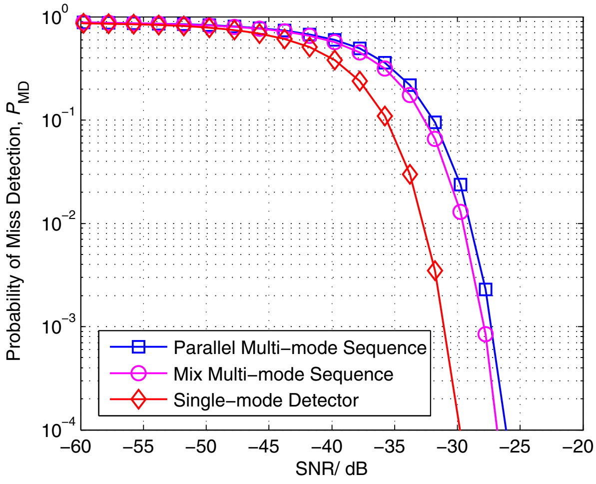

Fig. 7. Sensing performance of DTMB Mode 2 Signal when $N = 20$, $P_{\mathrm{FA}} = 10\%$.

Comparing with other modes of primary signals, MLS detectors suffer more performance degradation from receiving Mode 1 signal. The reason is that with the same number of received frames, the ENR of PN255 is lower than that of PN595 and PN511. Therefore Mode 1 signal is easier susceptible to the quasi-orthogonality of PN sequence.

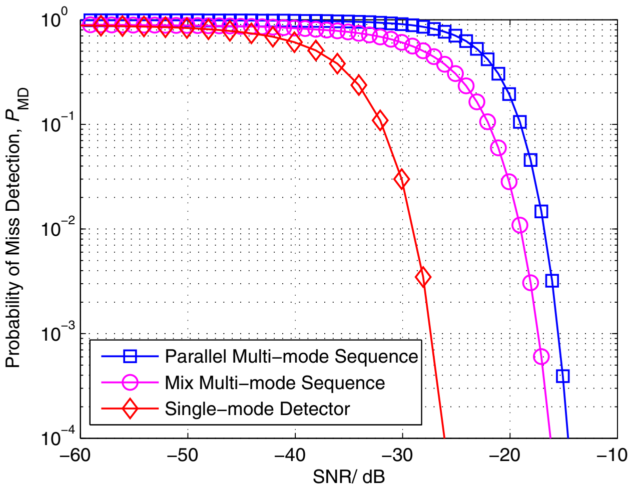

Fig. 8. Sensing performance of DTMB Mode 1 Signal when $N = 20$, $P_{\mathrm{FA}} = 10\%$.

5 Conclusion

In this paper, we have proposed two MLS detectors and their theoretical models for the DTMB multi-mode signal detection. The single-mode detector, which is derived from NP test, for the DTMB system was presented and thoroughly studied. The sensing performance of single-mode detector is the upper bound, which can be the benchmark for other detectors. The MLS multi-mode signal detectors, which are also based on Neyman-Pearson test, were fully investigated by quantitative analyses. The sensing performance was obtained through Monte Carlo simulations. Both simulation and theoretical analyses showed that MMLS and PMLS detectors can achieve the multi-mode signal detection. Due to the quasi-orthogonality of PN sequence, a tolerable performance loss of multi-mode detectors is not unavoidable.

References

1. Framing Structure, Channel Coding and Modulation for Digital Television Terrestrial Broadcasting System (2006)
2. Standard for Cognitive Wireless Regional Area Networks (RAN) for Operation in TV Band, July 2011
3. Chen, H.-S., Gao, W., Daut, D.G.: Spectrum sensing for DMB-T systems using PN frame headers. In: Proc. IEEE Int. Conf. Communications ICC 2008, pp. 4889–4893 (2008)
4. Federal Communication Commission, et al.: Second Report and Order and Memorandum Opinion and Order in the Matter of Unlicensed Operation in the TV Broadcast Bands Additional Spectrum for Unlicensed Devices Below 900 MHz and in the 3 GHz Band. Document, 260 (2008)
5. Kay, S.M.: Fundamentals of Statistical Signal Processing: Detection Theory, vol. ii, p. 7, Upper Saddle River, New Jersey (1998)
6. Lei, C., Jing, Q., Viessmann, A., Kocks, C., Bruck, G.H., Jung, P., Hu, R.Q.: A spectrum sensing prototype for tv white space in china. In: Proc. IEEE Global Telecommunications Conf., GLOBECOM 2011, pp. 1–6 (2011)
7. Mitola, J., et al.: Cognitive radio: An Integrated Agent Architecture for Software Defined Radio. Doctor of Technology, Royal Inst. Technol. (KTH), Stockholm, Sweden, pp. 271–350 (2000)
8. Shellhammer, S., Chouinard, G.: Spectrum Sensing Requirements Summary. IEEE P802 **22**, 802–822 (2006)
9. Song, J., Yang, Z., Yang, L., Gong, K., Pan, C., Wang, J., Wu, Y.: Technical Review on Chinese Digital Terrestrial Television Broadcasting Standard and Measurements on Some Working Modes **53**(1), 1–7 (2007)
10. Xu, A., Shi, Q., Yang, Z., Peng, K., Song, J.: Spectrum sensing for DTMB system based on PN cross-correlation. In: IEEE International Conference on Communications, pp. 1–5 (2010)
11. Yang, F., Peng, K., Song, J., Pan, C., Yang, Z.: Guard-interval mode detection method for the chinese DTTB system. In: Proc. Int. Conf. Communications, Circuits and Systems ICCCAS 2008, pp. 216–219 (2008)